Fiber laser-pumped, chirped, PPMgLN-based high efficient broadband mid-IR generation

Bo Wu (吴 波), Tao Chen (陈 滔), Jie Wang (王 杰), Peipei Jiang (姜培培), Dingzhong Yang (杨丁中), and Yonghang Shen (沈永行)*

State Key Laboratory of Modern Optical Instrumentation, Department of Optical Engineering, Zhejiang University, Hangzhou 310027, China

**Corresponding author: physyh@zju.edu.cn*

Received April 11, 2013; accepted May 13, 2013; posted online July 26, 2013

We demonstrate a high-efficiency, high-power-nanosecond fiber laser-pumped broadband mid-infrared output based on a linearly chirped PPMgLN crystal. By using a linearly polarized pulsed Yb-doped fiber laser as the pump, we experimentally obtain a 1.22-W broadband mid-infrared laser output under pump power of 10.15 W. The 3-dB bandwidths of the idler and signal output are approxiwately 150 and 13 nm, centering at 3.60 and 1.51 μm, respectively. The measured idler spectrum shows a smooth spectral profile.

OCIS codes: 190.4410, 190.4970

doi: 10.3788/COL201311.081901.

High-power broadband mid-infrared (IR) laser is of great interest in many applications, such as gas monitoring and highly sensitive chemical analysis. With the advantages of flexible grating structure design and the use of the highest nonlinear coefficient, periodically poled lithium niobate (PPLN) and/or aperiodically poled lithum niobate (APLN) are widely applied to the generation of broadband mid-IR laser. A feasible method to obtain broadband mid-IR laser output with a PPLN-based optical parametric oscillator (OPO) is to utilize a wide-bandwidth laser as the pump. In this way, Das *et al.* reported a 5.3-W, 63.7-cm^{-1} bandwidth idler output centering at 3 454 nm when pumping PPMgLN using a 73.9-cm^{-1} bandwidth continuous wave (CW) Yb fiber laser in 2009[1]. Another approach to obtain broadband mid-IR laser is to use a broadband phase-matched PPLN or APLN when pumped by a conventional narrow line-width laser. Short-length PPLN is typically used to generate broadband mid-IR laser through the methods of difference frequency generation (DFG) and optical parametnc amplifier (OPA). However, the short length and resultant low gain, of this PPLN limits the power output scalability. APLN, which is commonly optimized by using the simulated annealing method[2,3], is characterized by both high gain coefficient and broad phase-matching bandwidth, However, APLN has a complex design and is difficult to fabricate in such a manner as to obtain the desired domain structure with acceptable duty cycle.

In addition to PPLN and APLN, adiabatic PPLN[4] and two-dimensional (2D) designed PPLN[5] are also reported to generate broadband mid-IR laser, but the fabrication of these types of PPLN is likewise difficult.

Compared with the various PPLN/APLN types, the chirped PPLN is widely used in pulse compression, biphoton generation, broadband OPA, and femto-second OPOs[6-10]. The design and fabrication of the chirped PPLN is easier than that of APLN, and more importantly, the chirped PPLN retains the characteristics of both high gain coefficient and broad bandwidth.

Theoretical analysis shows that the chirped PPLN may exhibit a serious ripple phenomenon in its spectral output[11], which is not conducive to the generation of a well-shaped spectrum profile under high conversion efficiency in OPA and OPG. To mitigate this ripple phenomenon, the apodized PPLN is presented by changing the duty cycle of the gratings[12]. However, a disadvantage of this approach is that the change in duty cycle may result in a smaller conversion efficiency than that using the normal chirped PPLN.

Given its ease of design and fabrication, the chirped PPLN is typically used to generate broadband laser output under a femto-second laser pump[9,10]. However, the synchronous pumping condition required by the femto-second OPOs makes the whole system complex. The first nanosecond OPO based on a chirped PPMgLN was realized by Tillman *et al.* in 2007 when pumped by a Nd:YLF solid state laser with a 3-ns output pulse[13]. They obtained an approximately 20-mW mid-IR laser output around 3 220 nm when using a chirp structured PPMgLN. However, the spectrum of the mid-IR output was not specified.

In this letter, we report a fiber laser-pumped, linearly chirped, PPMgLN-based OPO for compact broadband mid-IR output. The fiber laser-pumped nanosecond OPOs represent a new generation of compact, high-power parametric devices for their excellent beam quality, simple thermal management schemes, and ultrahigh electrical-optical conversion efficiencies of such pump sources[14]. Several fiber laser-pumped OPO systems for the generation of high power mid-IR output by using home-made PPMgLN crystals but with limited spectral width have been previously demonstrated[15,16]. In this work, however, a linearly chirped PPMgLN is home fabricated and then used in the experiment to enable the generation of high-power, high-efficiency broadband mid-IR output power exceeding 1.2 W with a smooth spectral profile and a 3-dB bandwidth of 150 nm. This work is, to the best of our knowledge, the largest bandwidth high-power mid-IR laser in a nanosecond fiber laser-pumped chirped PPMgLN-based OPO.

The scheme of the experimental setup is shown in

Fig. 1. The chirped PPMgLN wafer was fabricated using a high-voltage trigging technique similar to that reported in Ref. [17]. The wafer was 50×15×1 (mm) in size, and had four-channels (CH0–CH3) with different chirping parameters. The width of each channel was 1.2 mm. The grating parameters of the chirped channels were derived from the formulation $\mathrm{sg}\{\cos[2\pi(a+bz)z]\}$, where z is the position of the crystal, $\mathrm{sg}(x)$ is a sign function, i.e., $\mathrm{sg}(x) = 1$ when $x > 0$; and $\mathrm{sg}(x)=-1$ when $x \leqslant 0$. The parameters a and b were 33 277.87 and 2 679.19 for channel 1 (CH1, corresponding to the grating period from 29.81 to 30.05 μm), 33 014.20 and 8 153.03 for channel 2 (CH2, corresponding to the grating period from 29.56 to 30.29 μm), and 32 765.40 and 13 642.93 for channel 3 (CH3, corresponding to the grating period from 29.30 to 30.52 μm). The channel 0 (CH0) was unchirped with a fixed period of 29.93 μm (see Fig. 2(a) for channel distribution) and used as the reference control. To illustrate the characteristics of the chirped PPMgLN, the Fourier transform of the phase matching frequencies in CH1 is shown in Fig. 2(b).

Both end facets of the PPMgLN wafer were finely polished and coated with antireflection films covering wavelengths of 3.2 to 4.0, 1.4 to 1.6 and 1.064 μm. The chirped PPMgLN was mounted on a copper base. When inserted into an OPO cavity, the crystal was oriented from a shorter to a longer grating period along the pump laser direction, i.e., the shorter grating period was close to the pump laser input end. Such orientation of the chirped PPMgLN was very important[13] for the broadband mid-IR generation, especially when the conversion efficiency of the OPO was high. The chirped PPMgLN-based OPO was designed as a double-pass single resonant cavity structure.

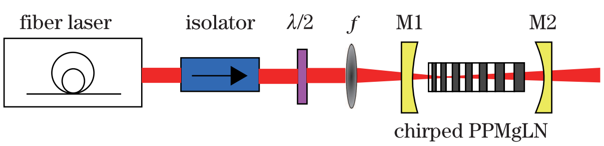

Fig. 1. Setup of chirped PPMgLN-based OPO for broadband mid-IR output.

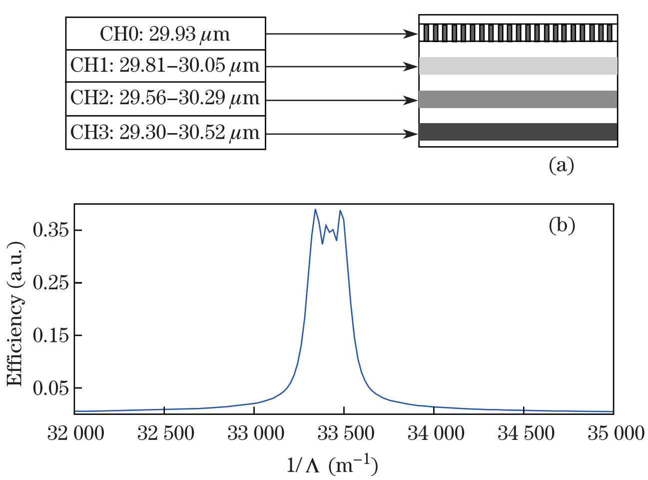

Fig. 2. (a) Grating structure of the chirped PPMgLN wafer. CH0 was unchirped for the reference control; CH1, CH2, and CH3 were designed with different chirp rates to generate 100-, 300- and 500-nm bandwidth mid-IR idlers respectively; (b) Fourier transform profile of the grating vector of CH1.

The cavity of the OPO was composed of two concave mirrors with cavity length of 60 mm. The input mirror, with a curvature of 500 mm, was coated for high transmissivity at 1.064 μm (T>95%), and high reflectivity from 1.4 to 1.6 μm (R >99%) and from 3.2 to 4.0 μm (R >99%), whereas the output coupler with a curvature of 200 mm was coated for high reflectivity at a wavelength of 1.064 and 1.4 to 1.6 μm (R >98%), high transmissivity from 3.2 to 4.0 μm.

The pump source used in the experiment was a master oscillator power amplifier structured linearly polarized pulsed Yb fiber laser, as previously reported in Ref. [18]. The bandwidth of the output fiber laser was approximately 0.5 nm. An optical isolator was placed between the fiber laser and the OPO to hinder the feedback of the pump laser from entering the OPO and prevent damage to the fiber laser. By using a single convex lens with a focusing length of 150 mm, the pump beam was focused into CH1. The focused pump beam diameter at waist was measured to be approximately 210 μm (measured by a beam profiler, high-power nanoscan HP-NS-PYR0/9/5, from Photon, Inc.), located at the one-third position of the cavity close to the input mirror. When the pump power was 10.15 W with a repetition rate of 40 kHz (the pulse width under this condition was approximately 75 ns), we obtained a 1.22-W broadband mid-IR laser output centering at 3.6 μm. This power was measured by directing the output of the OPO through a dichroic reflector, which allowed high reflection from 1.4 to 1.6 μm (R >99%) and high transmission from 3.2 to 4.0 μm (T >98%). The output power dependence of the mid-IR laser on the input pump power is shown in Fig. 3. The maximum conversion efficiency from the 1.06 μm pump laser to the broadband mid-IR was approximately 12.0%. Considering that the high reflection output coupler was used in the experiment, the slope efficiency was limited to approximately 16.6%.

Figure 4 illustrates the measured signal and the idler spectra of the OPO. The bandwidth of the signal (measured by an optical spectrum analyzer, AQ6375, with a resolution of 0.1 nm) was approximately 13 nm, with a rippled spectral profile quite similar to that obtained from theoretical design. The bandwidth of the corresponding idler (measured by Omni-λ 300 Spectrograph, Zolix, China with a resolution of 1 nm) was approximately 150 nm. However, the idler output exhibited a smooth differed shaped spectrum with negligible ripple, which completely from the

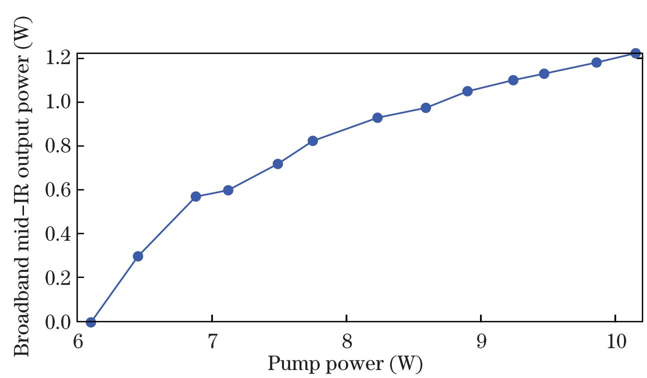

Fig. 3. Idler power dependence of the broadband mid-IR OPO on the pump power.

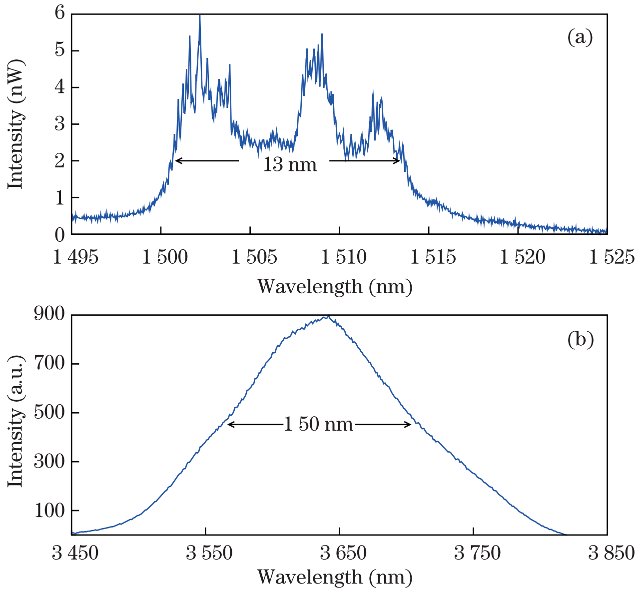

Fig. 4. Spectra of the broadband OPO output. (a) Spectrum of the signal. The bandwidth is 13 nm, similar to that from the theoretical analysis. The spectrum of the signal exhibites a ripple phenomenon; (b) spectrum of the idler. The band width is approximately 150 nm. Compared with the signal, the ripple phenomenon of the idler is negligible.

signal spectral profile. Comparing Figs. 4(a) and (b), the measured idler bandwidth in the experiment was evidently wider than that directly calculated from the measured signal spectrum. We attributed such difference of actual spectral width in the idler output from that calculated from the signal and pump spectra to the non-collinear phase-matching of the OPO, as mentioned in Ref. [16].

We also investigated the performance of CH2 with a wider idler output (designed for 300-nm bandwidth). However, we found that the wafer would likely break down with the occurence of OPO resonance even under the same pump condition as CH1. This problem became more serious when pumping the chirped channel 3 for 500-nm bandwidth mid-IR laser generation. We initially attributed this problem to the complex sum frequency generation that would produce a significaritly shorter wavelength or to the random coherent broadband laser pulse compression when pumped by a high peak power, long-pulse laser. Further investigation is necessary to clarify the mechanism involved.

In conclusion, we demonstrate a compact, linearly polarized, pulsed fiber laser-pumped, high-power, high-efficiency OPO with broadband mid-IR laser output. The conversion efficiency of the broadband mid-IR output at the maximum power of 1.22 W is approximately 12% with a 3-dB bandwidth of 150 nm and negligible ripple in spectrum. The techniques applied in this work can be used for the development of compact mid-IR laser with wider spectral output.

This work was supported by the National Natural Science Foundation of China (No. 61078015), National "973" Program of China (No. 2011CB311803), High Tech Program (No. 2009AA063006), Program of Zhejiang Province (No. 2010C31124), Zhejiang Provincial Natural Science Foundation of China (No. LQ12F05007), and the Educational Program of Zhejiang Province (No. Y200909758).

References

1. R. Das, S. C. Kumar, G. K. Samanta, and M. Ebrahim-Zadeh, Opt. Lett. **34,** 3836 (2009).
2. Y. Zhang and B. Y. Gu, Opt. Commum. **192,** 417 (2001).
3. X. Zeng, X. Chen, F. Wu, Y. Chen, Y. Xia, and Y. Chen, Opt. Commum. **204,** 407 (2002).
4. H. Suchowski, D. Oron, A. Arie, and Y. Silbergerg, Phys. Rev. A **78,** 063821 (2008).
5. P. Ni, B. Ma, X. Wang, B. Cheng, and D. Zhang, Appl. Phys. Lett. **82,** 4230 (2003).
6. X. Zeng, S. Ashihara, X. Chen, T. Shimura, and K. Kuroda, Opt. Commum. **281,** 4499 (2008).
7. M. B. Nasr, S. Carrasco, B. E. A. Saleh, A. V. Sergienko, M. C. Teich, and J. P. Torres, Phys. Rev. Lett. **100,** 183601 (2008).
8. S. Sensam, G. Y. Yin, and S. E. Harris, Phys. Rev. Lett. **104,** 253602 (2010).
9. M. Charbonneau-Lefort, B. Afeyan, and M. M. Fejer, J. Opt. Soc. Am. B **25,** 1402 (2008).
10. C. Heese, C. R. Phillips, L. Gallmann, M. M. Fejer, and U. Keller, Opt. Lett. **35,** 2340 (2010).
11. M. Charbonneau-Lefort, B. Afeyan, and M. M. Fejer, J. Opt. Soc. Am. B **25,** 463 (2008).
12. T. Umeki, M. Asobe, T. Yanagawa, O. Tadanaga, Y. Nishida, K. Magari, and H. Suzuki, J. Opt. Soc. Am. B **26,** 2315 (2009).
13. K. A. Tillman and D. T. Reid, Opt. Lett. **32,** 1548 (2007).
14. D. J. Richardson, J. Nilsson, and W. A. Clarkson, J. Opt. Soc. Am. B **27,** B63 (2010).
15. Y. Shen, S. U. Alam, K. K. Chen, D. Lin, S. Cai, B. Wu, P. Jiang, A. Malinowski, and D. J. Richardson, IEEE J. Sel. Top. Quantum Electron. **15,** 385 (2009).
16. D. Lin, S. Alam, Y. Shen, T. Chen, B. Wu, and D. J. Richardson, Opt. Express **20,** 15008 (2012).
17. B. Wu, J. Kong, and Y. Shen, Opt. Lett. **35,** 1118 (2010).
18. P. P. Jiang, D. Z. Yang, Y. X. Wang, T. Chen, B. Wu, and Y. H. Shen, Laser Phys. Lett. **6,** 384 (2009).